Inorg. Chem. **2005**, *44*, 9416–9423

Inorganic–Organic Hybrids of the *p*,*p*′-Diphenylmethylenediphosphinate, pcp^{2-}. Synthesis, Characterization, and XRPD Structures of [Sn(pcp)] and [Cu(pcp)]

Jens Beckmann,[†,‡] Ferdinando Costantino,[§] Dainis Dakternieks,[†] Andrew Duthie,[†] Andrea Ienco,[∥] Stefano Midollini,[∥] Cassandra Mitchell,[†] Annabella Orlandini,*[,∥] and Lorenzo Sorace[⊥]

Istituto di Chimica dei Composti Organometallici, ICCOM, CNR, Via Madonna del Piano, 50019 Sesto Fiorentino, Firenze, Italy, Dipartimento di Chimica, Università di Perugia, Via Elce di Sotto 8, 06123 Perugia, Italy, Centre for Chiral and Molecular Technologies, Deakin University, Geelong, Victoria 3217, Australia, and Dipartimento di Chimica and UdR INSTM, Università di Firenze, Via della Lastruccia 3, 50019 Sesto Fiorentino, Firenze, Italy

Received May 3, 2005

Two new inorganic–organic polymeric hybrids [Sn(pcp)] and [Cu(pcp)], pcp = $CH_2(PhPO_2)_2^{2-}$, have been synthesized and structurally chracterized. The tin derivative has been obtained by reaction of the *p*,*p*′-diphenylmethylenediphosphinic acid (H_2pcp) in water with $SnCl_2 \cdot 2H_2O$, while the copper derivative has been synthesized through a hydrothermal reaction from the same H_2pcp acid and $Cu(O_2CMe)_2 \cdot H_2O$. The structures of these compounds have been solved "ab initio" by X-ray powder diffraction (XRPD) data. [Sn(pcp)] has a ladder-like polymeric structure, with tin(II) centers bridged by diphenylmethylenediphosphinate ligands, and alternating six- and eight-membered rings. The hemilectic coordination around the metal shows the tin(II) lone pair to be operative, resulting in significant interaction mainly with a C–C bond of one phenyl ring. The [Cu(pcp)] complex displays a polymeric columnar structure formed by two intersecting sinusoidal ribbons of copper(II) ions bridged by the bifunctional phosphinate ligands. The intersections of the ribbons are made of dimeric units of pentacoordinated copper ions. Crystal data for [Sn(pcp)]: monoclinic, space group $P2_1/c$, $a = 11.2851(1)$, $b = 15.4495(6)$, $c = 8.6830(1)$ Å, $\beta = 107.546(1)°$, $V = 1443.44(9)$ Å, $Z = 4$. Crystal data for [Cu(pcp)]: triclinic, space group $P\bar{1}$, $a = 10.7126(4)$, $b = 13.0719(4)$, $c = 4.9272(3)$ Å, $\alpha = 92.067(5)$, $\beta = 95.902(7)$, $\gamma = 87.847(4)°$, $V = 685.47(7)$, $Z = 2$. The tin compound has been characterized by ^{119}Sn MAS NMR (magic-angle spinning NMR), revealing asymmetry in the valence electron cloud about tin. Low-temperature magnetic measurements of the copper compound have indicated the presence of weak antiferromagnetic interactions below 50 K.

Introduction

Hybrid organic−inorganic metal complexes are a versatile class of materials, well-suited to structural design, by modulation of both the ionic framework and the organic constituent. Metal organic-phosphonate/phosphinates represent a very important series, as they have found application in various fields (catalysis, ion exchange, material science, optics, and magnetism).[1,2] Whereas a plethora of metal phosphonates, with a variety of structural arrangements and dimensionality, have been reported (see examples in refs 3−8), the number of metal phosphinates described is limited (see examples in refs 9 and 10). This is most likely due to

* To whom correspondence should be addressed. E-mail: annabella.bianchi@iccom.cnr.it.
[†] Centre for Chiral and Molecular Technologies, Deakin University.
[‡] Present address: Institut für Chemie, Freie Universität Berlin, Fabeckstrasse 34-36, 14195 Berlin, Germany.
[§] Dipartimento di Chimica, Università di Perugia.
[∥] Istituto di Chimica dei Composti Organometallici, CNR.
[⊥] Dipartimento di Chimica, Università di Firenze.

(1) Vioux, A.; Le Bideau, J.; Mutin, P. H.; Leclercq, D. *Top. Curr. Chem.* **2004**, *232*, 145−174 and references therein.
(2) Allcock, H. R. *Adv. Mater.* **1994**, *6*, 106−115.
(3) Thompson, M. E. *Chem. Mater.* **1994**, *6*, 1168−1175.
(4) Clearfield, A. *Curr. Opin. Solid State Mater. Sci.* **2002**, *6*, 268−278.
(5) Clearfield, A. *Curr. Opin. Solid State Mater. Sci.* **2002**, *6*, 495−506.
(6) Bakhmutova, E. V.; Ouyang, X.; Medvedev, D.G.; Clearfield, A. *Inorg. Chem.* **2003**, *42*, 7046−7051.
(7) Stock, N.; Frey, S. A.; Stucky, G. D.; Cheetham, A. K. *J. Chem. Soc., Dalton Trans.* **2000**, 4292−4296.
(8) Burlholder, E.; Golub, V. O.; O'Connor, C. J.; Zubieta, J. *Inorg. Chim. Acta* **2002**, *340*, 127−132.

10.1021/ic050683p CCC: $30.25
Published on Web 11/02/2005

Chart 1

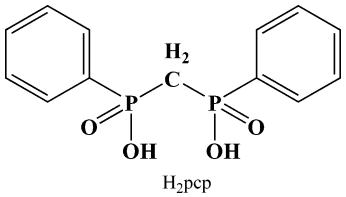

H_2pcp

the perception of there being less potentiality for building up extended structures. However, recently we have exploited the ligand capacity of the bifunctional *p*,*p*′diphenylmethylenediphosphinate ligand, pcp^{2-} (Chart 1),[11] which, as far as we know, has only previously been used once, to prepare a metal complex, namely polymeric $Ti(pcp)_2$, which was of unspecified structure.[12] This pcp^{2-} dianion contains four oxygen donor atoms, potentially allowing the coordination of a single metal ion (either with one or two oxygens) and/or bridging of multiple metal centers. Only the chelation of a single metal ion by the two oxygens at the same PO_2 seems to be excluded because of the large bite angle. Therefore, the formation of pcp−metal complexes displaying a remarkable array of different structural arrangements could be expected.

As a matter of fact, we have successfully prepared and characterized hybrid polymers with different metal ions(II), like Be(II),[13] Mn(II),[14] Co(II),[14] Ni(II),[14] Cu(II),[15] Zn(II), [16] and Pb(II).[17] In particular, the anhydrous [Zn(pcp)] and [Pb(pcp)] complexes present polymeric arrangements, characterized, respectively, by 2D layered and 1D columnar structures. All the other complexes so far isolated contain water solvent molecules. Nickel, cobalt, and manganese give rise to the isomorphous series $[M(pcp)(H_2O)_3]\cdot H_2O$, where the structure is arranged in the form of 2D hydrogen-bonded layers.[14] An analogous structural network has been found for the $[Cu(pcp)(H_2O)_2]\cdot H_2O$ complex. It is worth noting the role played by the crystallization and coordination water molecules in these hydrated materials, which controls the extended architecture via the networks of hydrogen-bonding interactions.[15] The cementing power of the hydrogen bonding is also exemplified in the extended $[Be(pcp)(H_2O)_2]$ derivative, where each pcp^{2-} anion chelates one metal center.[13]

Now we report the synthesis and characterization of two new anhydrous pcp polymers containing the tin(II) and copper(II) ions, namely [Sn(pcp)] and [Cu(pcp)].The absence of crystallization and coordination water in these two compounds seems to be determinant not only for the dimensionality but also for the rate of crystal growth. These solids are, in fact, microcrystalline, and it was only possible to characterize their structures thanks to the application of the "ab initio" X-ray powder diffraction (XRPD) methods, which represent a powerful analytical tool when single crystals are not available. A ^{119}Sn MAS NMR (magic-angle spinning NMR) study has been performed on the tin complex, whereas magnetic measurements were carried out on the copper derivative.

Experimental Section

Materials and Methods. All reagents were analytical-grade commercial products and were used without further purification. The *p*,*p*′-diphenylmethylenediphosphinic acid (H_2pcp) was prepared as previously described.[11,15] The hydrothermal reactions were performed in a stainless steel autoclave, with a Teflon insert (ca. 20 mL capacity), constructed in-house.

Synthesis of [Sn(pcp)], 1. A suspension of $SnCl_2\cdot 2H_2O$ (500 mg, 2.22 mmol) and $CH_2(PhP(O)(OH))_2$ (H_2pcp) (656 mg, 2.22 mmol) was refluxed for 12 h in water. The solution was filtered while still hot, before approximately one-third of the water was removed in a vacuum. Upon cooling, a colorless precipitate formed, which was filtered, washed with water, and dried in a vacuum. Yield 810 mg, 88%. mp > 300 °C. Anal. Calcd for $C_{13}H_{12}O_4P_2Sn$: C, 37.81; H, 2.93. Found: C, 37.20; H, 2.76%.

Synthesis of [Cu(pcp)], 2. The hydrothermal reaction of $Cu(O_2CMe)_2\cdot H_2O$ (27 mg, 0.135 mmol) and H_2pcp (40 mg, 0.135 mmol) in 6 mL of H_2O, at 453 K for 3 days, followed by slow cooling at room temperature, produced thin pale-blue crystals of the complex. The compound was filtered, washed with water, and dried in air, at room temperature.The complex is insoluble in water, where it remains unchanged (any of the two hydrated $[Cu(pcp)(H_2O)_2]\cdot H_2O$ and $[Cu(pcp)(H_2O)_2]$ complexes, previously synthesized by conventional reactions, cannot be obtained starting from the title complex).[15] Yield 31 mg, 64%. Anal. Calcd for $C_{13}H_{12}CuO_4P_2$: C, 43.65; H, 3.38. Found: C, 43.58; H, 3.45.

X-ray Powder Diffraction Analysis. An X-ray powder diffraction pattern of [Sn(pcp)] was collected using a Bruker D8 advance powder diffractometer, equipped with Cu Kα radiation and operating in $\theta-2\theta$ Bragg Brentano geometry at 40 kV and 30 mA. The "SolX" solid-state detector was used. 0.8 mm divergence, 0.2 antiscatter, and 0.1 mm receiving slits were used. C/Ni Goebel mirrors for the incident beam were used. The X-ray powder diffraction pattern of [Cu(pcp)] was collected using a Philips XPERT APD PW 3020 goniometer, using the Bragg−Brentano $\theta-2\theta$ geometry and equipped with Cu Kα radiation and a bent graphite monochromator on the diffracted beam. The LFF tube operated at 40 kV, 30 mA. To minimize preferred orientations, the sample was carefully side-loaded onto an aluminum sample holder with an oriented quartz monocrystal underneath. The diffraction patterns for [Sn(pcp)] and [Cu(pcp)] were fitted using a Pearson VII profile function, and the position of the first 20 lines ($K\alpha_1$ maxima) was used for the indexing procedures. Indexing procedures were performed using the TREOR program[18] giving a monoclinic cell [M(20) = 18, F(20) = 49] for **1** and a triclinic cell [M(20) = 13, F(20) = 32][19] for **2** as the best solutions. Their cell parameters are shown in Table 1. Systematical absences of the class *0k0*, *k* =

(9) Grohol, D.; Ginge, F.; Clearfield, A. *Inorg. Chem.* **1999**, *38*, 751−756.
(10) Oliver, K. W.; Rettig, S. J.; Thomson, R. C.; Trotter, J.; Xuia, S. *Inorg. Chem.* **1997**, *36*, 2465−2468.
(11) Garst, M. E. *Synth. Commun.* **1979**, *9*, 261−266.
(12) Dahl, G. H.; Block, P. B. *Inorg. Chem.* **1966**, *5*, 1394−1396.
(13) Cecconi, F.; Dominguez, S.; Masciocchi, N.; Midollini, S,; Sironi, A.; Vacca, A. *Inorg. Chem.* **2003**, *42*, 2350−2356.
(14) Berti, E.; Cecconi, F.; Ghilardi, C. A.; Midollini, S.; Orlandini, A.; Pitzalis, E. *Inorg. Chem. Commun.* **2002**, *5*, 1041−1043.
(15) Ciattini, S.; Costantino, F.; Lorenzo-Luis, P.; Midollini, S.; Orlandini, A.; Vacca, A. *Inorg. Chem.* **2005**, *44*, 4008−4016.
(16) Cecconi, F.; Dakternieks, D.; Duthie, A.; Ghilardi, G. A.; Gili, P.; Lorenzo-Luis, P. A.; Midollini, S.; Orlandini, A. *J. Solid State Chem.* **2004**, *177*, 786−792.
(17) Cecconi, F.; Ghilardi, C. A.; Midollini, S.; Orlandini, A. *Inorg. Chem. Commun.* **2003**, *6*, 546−548.
(18) de Wolff, P. M. *J. Appl. Crystallogr.* **1968**, *1*, 108−113.
(19) Werner, P. E.; Eriksson, L.; Westdhal, M. *J. Appl. Crystallogr.* **1985**, *18*, 367−370.

Table 1. Crystal Data and Refinement Details for **1** and **2**

	1	**2**
empirical formula	$C_{13}H_{12}O_4P_2Sn$	$C_{13}H_{12}O_4P_2Cu$
fw	412.87	357.63
cryst syst	monoclinic	triclinic
space group	$P2_1/c$	$P\bar{1}$
a/Å	11.2851(1)	10.7126(4)
b/Å	15.4495(6)	13.0719(4)
c/ Å	8.6830(1)	4.9272(3)
α/deg	107.546 (1)	92.067(5)
β/deg		95.902(7)
γ/deg		87.847(4)
vol/Å^3	1443.44 (9)	685.47(4)
Z	4	2
T/°C	25	25
calcd density/g·cm^{-3}	1.84	1.67
pattern range, 2θ/deg	7.5−100	3−130
step scan increment, 2θ/deg	0.01	0.02
step scan time/s	15	30
no. of data points	10547	6296
no. of reflns	4162	2600
no. of params	71	90
no. of restraints	56	70
R_p[a]	0.075	0.053
R_{wp}[b]	0.096	0.037
R_F^2[c]	0.084	0.054
χ[d]	1.56	5.07

[a] $R_p = \sum|I_o - I_c|/\sum I_o$. [b] $R_{wp} = [\sum w(I_o - I_c)^2/\sum wI_o^2]^{1/2}$. [c] $R_F^2 = \sum|F_o^2 - F_c^2|/\sum|F_o^2|$. [d] $\chi = [\sum w(I_o - I_c)^2/(N_o - N_{var})]^{1/2}$

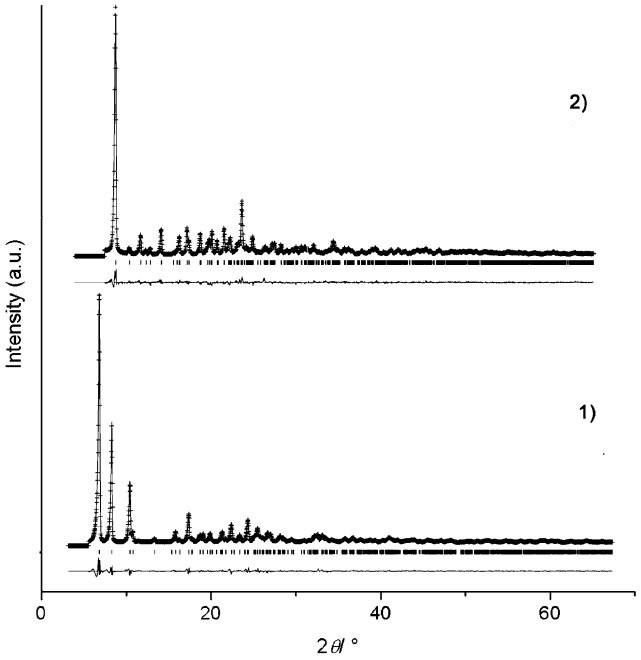

Figure 1. Rietveld plots for **1** and **2** in the 3−70 2ϑ region. Calculated, observed, and differences curves are shown.

$2n + 1$, and $h0l$, $l = 2n + 1$, suggested $P2_1/c$ as the best space group for **1**. Structural determination for **1** and **2** was performed using the FOX program.[20] The program optimizes a structural model described by the use of building blocks defined in terms of their internal coordinates, such as bond lengths, bond angles, and dihedral angles. Optimization was performed by comparing the XRPD patterns calculated from randomly generated configurations and using the "integrated R_{wp}" (iR_{wp}) as the cost function. Trial structures were generated using the "Parallel Tempering" algorithm.[21] The starting model was composed by the free metal atom and the pcp^{2-} diphosphinic group. Hydrogen atoms were omitted. Starting values for bond lengths and angles were taken from similar systems found in the literature and constrained within a standard deviation of 0.15 Å and 10°, respectively. Internal bond lengths and angles were not optimized. All other dihedral angles were left to change freely. Antibump restraints (distance M−P = 2.6(5) Å) between the metal and the phosphorus atoms were fixed in order to speed up the optimization process. Rietveld refinement of the structures was performed using the GSAS program (see Figure 1).[22] First of all, zero shift, cell parameters, background, and profile shape were refined. A pseudo voigt profile function[23] (six terms) with two terms for the correction of asymmetry at the low-angle region was used.[24] Then atomic coordinates and isotropic thermal factors were refined. The following soft restraints between all the atoms were imposed: Sn−O = 2.05(5), P−O = 1.56(5), and P−C = 1.83(5) Å for **1** and Cu−O = 1.95(5), P−O = 1.56(5), and P−C = 1.83(5) Å for **2**, and the "ideal planar ring" restraint for the phenyl groups was used (C−C distance = 1.39(5) Å and aromatic bond angles = 120(1)°). The statistical weight of these restraints was maintained to a relatively high value as the refinement proceeded, and it was not possible to set it to zero because of some unrealistic light atom bond distances. Thermal factors were refined only for metals and P atoms, while those of light atoms were set at a fixed value and were not refined.

MAS NMR Measurements. The MAS NMR spectra were measured using a Joel Eclipse Plus 400 spectrometer (at 161.84 (^{31}P) and 149.05(^{119}Sn)) equipped with a 6 mm MAS probe. Crystalline $NH_4H_2PO_4$ (δ 0.95) and c-Hex$_4$Sn (δ −97.35) were used as secondary references against aqueous H_3PO_4 (90%) and SnMe$_4$. The ^{119}Sn MAS NMR spectra were obtained using cross-polarization (contact time 5 ms and recycle delay 10 s). A tensor analysis was performed on the ^{119}Sn MAS NMR data using the computer program DM Fit 2002[25] and was based on relative intensities of the spinning sidebands. Definitions are δ_{iso} (ppm) = $-\sigma_{iso}$ = $-(\sigma_{11}+\sigma_{22}+\sigma_{33})/3$; ζ (ppm) = $\sigma_{33} - \sigma_{iso}$ and $\eta = (\sigma_{22} - \sigma_{11})/(\sigma_{33} - \sigma_{iso})$, where σ_{11}, σ_{22}, and σ_{33} are the principal tensor components of the shielding anisotropy (SA), sorted as follows $|\sigma_{33} - \sigma_{iso}| > |\sigma_{11} - \sigma_{iso}| > |\sigma_{22} - \sigma_{iso}|$. ^{31}P MAS NMR δ: 19.5, 18.3. ^{119}Sn MAS NMR δ_{iso}: −685.0; ζ: 484; η: 0.40; σ_{11}: 346; σ_{22}: 540; σ_{33}: 1169.

Magnetic Measurements. Magnetic susceptibility of a sample powder of [Cu(pcp)] was measured between 2 and 300 K with applied magnetic fields of 1 T using a Cryogenic S600 SQUID magnetometer. Data were corrected for the magnetism of the sample holder, which was determined separately in the same temperature range and field, and the underlying diamagnetism of each sample was estimated from Pascal's constants. Magnetization measurements were performed on the same sample at 1.8 K with a field up to 6.5 T. An electron paramagnetic resonance (EPR) spectrum was recorded with an X-Band Bruker Elexsys E500 spectrometer.

(20) Favre-Nicolin, V.; Cerny, R. *J. Appl. Crystallogr*. **2002**, *35*, 734−743.
(21) Falcioni, M.; Deem, M. W. *J. Chem. Phys*. **1999**, *110*, 1754−1766.
(22) Larson, A. C.; von Dreele, R. B. *Generalized Crystal Structure Analysis System*; Los Alamos National Laboratory: Los Alamos, NM, 2001.
(23) Thompson, P.; Cox, D. E.; Hastings, J. B. *J. Appl. Crystallogr*. **1987**, *20*, 79−83.
(24) Finger, L. W.; Cox, D. E.; Jephcoat, A. P. *J. Appl. Crystallogr*. **1994**, *27*, 892−900.
(25) Massiot, D.; Fayon, F.; Capron, M.; King, I.; Le Calvè, S.; Alonso, B.; Durand, J.-O.; Bujoli, B.; Gan, Z.; Hoatson, G. *Magn. Reson. Chem*. **2002**, *40*, 70−76.

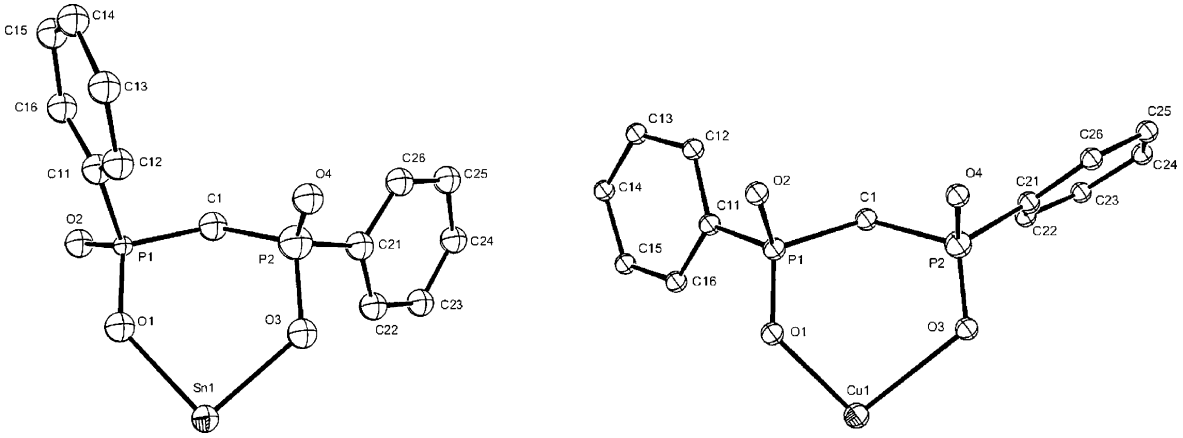

Figure 2. Perspective view of the asymmetric units of [Sn(pcp)] **1** (left) and [Cu(pcp)] **2** (right) polymers. ORTEP drawing with 30% probability ellipsoids.

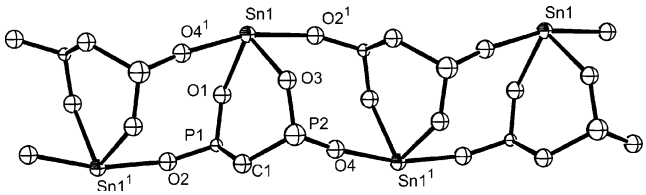

Figure 3. Propagation of the polymer of [Sn(pcp)] along the *z* direction. Phenyl rings omitted for sake of clarity.

Results and Discussion

Descriptions of the Structures. The X-ray study of [Sn(pcp)] and [Cu(pcp)] revealed polymeric structures for both the compounds. Their asymmetric units are similar (Figure 2), with the only significant difference being the relative orientation of the phenyl rings, which are in the anti- and syn-positions in **1** and **2**, respectively.

Despite having similar building units, the unique nature of the two metal ions results in different processes of building up of the extended networks. In particular in **1**, each tin center is surrounded by four oxygens atoms from three pcp^{2-} ligands, with one acting as bidentate and the other two acting as monodentate, with each pcp^{2-} ligand bridging three metals ions. This results in a one-dimensional ribbon, where six-membered Sn−O−P−C−P−O rings alternate with eight-membered Sn−O−P−O−Sn−O−P−O rings, forming an undulated ladder-like structure. The open space between the ribbons is reduced by the presence of the organic part of the ligand, namely, the phenyl rings, and additionally by the tin(II) ion lone pair, whose presence is well-inferred from the hemilectic coordination around the metal (Figures 3 and 4). As a matter of fact, if we assume the $O2^1$-Sn−$O4^1$ as one trans basal angle, the tin(II) coordination sphere resembles a distorted square pyramid, missing the fifth donor in the basal plane. The lone pair should be likely positioned opposite to the O3 donor, which actually displays the shortest Sn−O bond (2.074(7) Å) (see Table 2). The Sn−O bond lengths, ranging from 2.074 to 2.162 Å, are similar to analogous distances reported in the literature.[26−30] The truncated square pyramidal Sn(II) coordination sphere SnO_4E

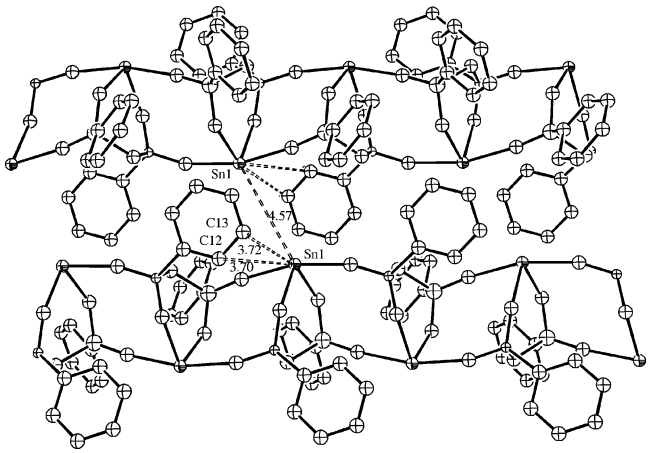

Figure 4. Portion of the polymer of [Sn(pcp)] showing the likely interactions interesting the lone pair of tin(II), viewed normal to [100].

(E = electron pair) has been described in other tin(II) polymeric phosphates and phosphonates complexes: see, for examples, $[Sn(O_3PCH_2PO_3]^{2-}$,[26] $Sn_4(O_3PCH_2CH_2CO_2)_2(C_2O_4)$,[27] and $Sn_2(PO_4)(C_2O_4)_{0.5}$.[28]

In considering the activity of the tin(II) lone pair, it seems to be likely pointing toward the C12−C13 bond of the P1 phenyl ring, with distances Sn···C of 3.70 and 3.72 Å, respectively, suggesting that there is some interaction (sum of the van der Waals = 3.87 Å). This interaction does not contribute to extending the structure dimensionality, because it involves the lone pair and one phenyl ring of the same ribbon (Figure 4). Anyway, if we consider the *inter*-ribbon Sn···Sn separation of 4.57 Å (only slightly larger than the sum of the van der Waals radii (4.34 Å), a lone pair pointing toward the tin of the adjacent ribbon could not be excluded. In this case, the coordination sphere including the lone pair would be better described as trigonal bipyramidal rather than square pyramidal. In a recent paper by some of us, interactions between Te and the $C(sp^2)$−$C(sp^2)$ bonds of two individual phenyl rings have been observed, which are due

(26) Adair, B. A.; Neeraj, S.; Cheetham, A. K. *Chem. Mater*. **2003**, *15*, 1518−1529.

(27) Stock, N.; Stucky, G. D.; Cheetham, A. K. *Chem. Commun*. **2000**, 2277−2278.

(28) Natarajan, S. *J. Solid State Chem*. **1998**, *139*, 200−203.

(29) Zapf, P. J.; Rose, D. J.; Haushalter, R. C.; Zubieta, J. *J. Solid State Chem*. **1996**, *125*, 182−185.

(30) Zapf, P. J.; Rose, D. J.; Haushalter, R. C.; Zubieta, J. *J. Solid State Chem*. **1997**, *132*, 438−442.

Table 2. Selected Bond Distances (Å) and Angles (deg) for **1**[a]

bond	distance	bond	angle
Sn1−O1	2.118(6)	O1−Sn1−O2#1	98.3(6)
Sn1−O2#1	2.127(6)	O1−Sn1−O3	85.6(5)
Sn1−O3	2.074(7)	O1−Sn1−O4#2	72.0(3)
Sn1−O4#2	2.162(6)	O2#1-Sn1−O3	73.3(3)
P1−O1	1.482(8)	O2#1-Sn1−O4#2	164.1(5)
P1−O2	1.494(8)	O3−Sn1−O4#2	93.0(5)
P1−C1	1.783(7)	O1−P1−O2	114.8(7)
P1−C11	1.759(7)	O1−P1−C1	109.2(5)
P2−O3	1.550(8)	O1−P1−C11	110.1(6)
P2−O4	1.457(7)	O2−P1−C1	106.9(6)
P2−C1	1.762(7)	O2−P1−C11	110.2(6)
P2−C21	1.767(6)	C1−P1−C11	105.2(9)
		O3−P2−O4	111.7(6)
		O3−P2−C1	108.8(6)
		O3−P2−C21	102.9(5)
		O4−P2−C1	113.3(6)
		O4−P2−C21	115.8(6)
		C1−P2−C21	103.5(4)
		Sn1−O1−P1	141.6(6)
		Sn1−O2−P1	155.7(6)
		Sn1−O3−P2	137.5(7)
		Sn1−O4−P2	172.4(9)
		P1−C1−P2	118.2(6)

[a] Symmetry transformations used to generate equivalent atoms: #1, x, $-y + {}^3/_2$, $z - {}^1/_2$; #2, x, $-y + {}^3/_2$, $z + {}^1/_2$.

Table 3. Selected Bond Distances (Å) and Angles (deg) for **2**[a]

bond	distance	bond	angle
Cu1−O1	2.019(13)	O1−Cu1−O2#1	89.5(6)
Cu1−O2#1	1.885(12)	O1−Cu1−O3	95.3(7)
Cu1−O3	2.411(12)	O1−Cu1−O3#2	173.1(7)
Cu1−O3#2	1.942(11)	O1−Cu1−O4#3	85.7(6)
Cu1−O4#3	1.965(11)	O2#1−Cu1−O3	93.3(6)
P1−O1	1.438(10)	O2#1−Cu1−O3#2	95.9(6)
P1−O2	1.506(11)	O2#1−Cu1−O4#3	175.0(4)
P1−C1	1.843(10)	O3−Cu1−O3#2	89.4(6)
P1−C11	1.810(10)	O3−Cu1−O4#3	89.5(6)
P2−O3	1.444(10)	O3#2−Cu1−O4#3	88.6(6)
P2−O4	1.518(11)	O1−P1−O2	121.1(10)
P2−C1	1.842(11)	O1−P1−C1	109.4(9)
P2−C21	1.763(10)	O1−P1−C11	107.9(9)
		O2−P1−C1	107.8(9)
		O2−P1−C11	108.0(8)
		C1−P1−C11	100.8(6)
		O3−P2−O4	115.1(10)
		O3−P2−C1	111.4(11)
		O3−P2−C21	114.2(8)
		O4−P2−C1	103.5(7)
		O4−P2−C21	106.5(7)
		C1−P2−C21	105.1(6)
		Cu1−O1−P1	132.0(11)
		Cu1−O2−P1	131.9(9)
		Cu1−O3−P2	144.5(11)
		Cu1−O4−P2	140.9(9)
		P1−C1−P2	116.2(7)

[a] Symmetry transformation used to generate equivalent atoms: #1, x, y, $z - 1$; #2, $-x + 2$, $-y + 1$, $-z$; #3, $-x + 2$, $-y + 1$, $-z + 1$.

to the lone pair on Te.[31] Finally, additional contacts in the range 3.7−4.0 Å are present between P1- and P2-phenyl groups belonging to adjacent polymeric units. The complete packing diagram with view normal to [001] is reported in Figure S1 (in Supporting Information).

The copper derivative [Cu(pcp)] **2** has a polymeric monodimensional structure, formed by two intersecting undulated ribbons of Cu atoms bridged by the phosphinate

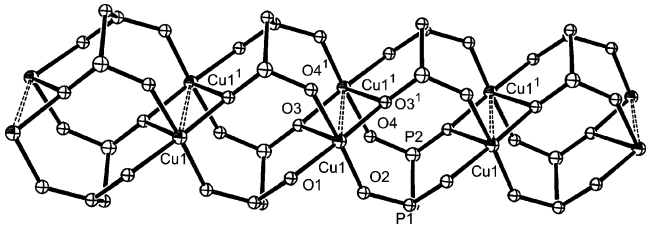

Figure 5. Propagation of the polymer of [Cu(pcp)] along the z direction. Phenyl rings omitted for sake of clarity.

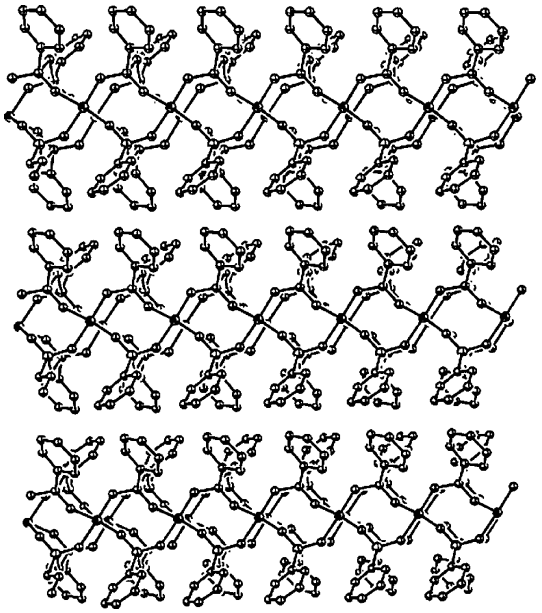

Figure 6. Portion of the polymer of [Cu(pcp)], showing the packing of the strands, with phenyl groups included (best view).

ligand. The intersections of the ribbons are constituted by dimeric units of copper(II) ions, which display a Cu···Cu separation of ca. 3.1 Å. Each copper center is five-coordinated, being surrounded by five oxygens from four different pcp^{2-} ligands to give a square pyramidal geometry. In turn, each phosphinate links four copper atoms, using all of its four oxygen donors in monodentate or bidentate fashion. The propagation of the polymer along the z direction is given in Figures 5 and 6. The complete packing diagram of [Cu(pcp)] with view normal to [001] is reported in Figure S2 (in Supporting Information), revealing the stacked arrangement of phenyl groups, which project into the voids between the polymeric strands.

A structural framework analogous to the copper structure has been recently reported for the lead(II) polymer [Pb(pcp)],[16] which shows the same polymeric array and packing but some differences in the first coordination sphere of the metal, because of the presence of an operative electron lone pair on the lead atom. Bond distances and angles within the coordination sphere of **2** (see Table 3) are instead in agreement with those found in the hydrated $[Cu(pcp)(H_2O)_2]\cdot H_2O$ and [Cu(pcp)(bipy)(H_2O)] compounds, where the presence of water molecules extends the dimensionality through hydrogen-bonding interactions.[15] The major difference observed in the latter complexes with respect to the dehydrated copper compound is the shorter length of the Cu−O apical bond (Cu−O_{ap} 2.215(6) and 2.174(4) versus 2.411(12) Å,

(31) Beckmann, J.; Dakternieks, D.; Duthie, A.; Mitchell, C.; Schürmann, M. *Aust. J. Chem*. **2005**, *58*, 119−127.

Chart 2

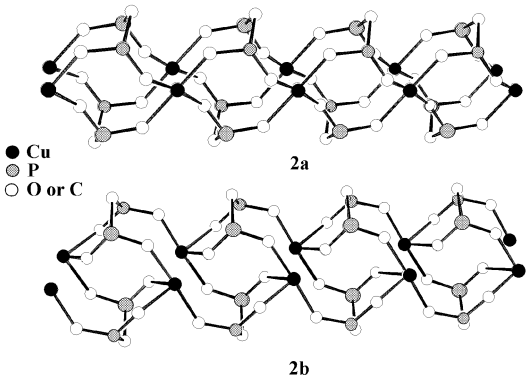

respectively). The fact is not surprising, if we consider that the oxygen positioned in apical position in the title compound is shared between the two copper atoms of a dimeric subunit.

Finally, the fact that the isostructural copper and lead derivatives display completely different structures compared to the related tin polymer could be explained considering that the $5s^2$ lone pair of tin(II) is stereochemically more active than the $6s^2$ lone pair of lead(II) (the stereochemical activity of the lone pair is more important for small cations than for big cations: it increases going up a group in the periodic table, in agreement with the evolution of the covalent character of the elements). In this context, the stereochemical requirement of the lone pair on tin(II) seems be important in the construction of the polymer, preventing a more compact structure. Finally, the [Zn(pcp)] hybrid material recently reported[16] displays a 2D layered structure, completely different from the networks found in the tin, lead, and copper derivatives.

Topological Analysis of the 1 and 2 Networks.We have wondered whether **1** and **2** complexes are topologically equivalent or not, that is, whether an interconversion between their skeletons is possible. With this in mind, we have potentially reduced the two metal centers at the same coordination number, breaking up one Cu−O bond, namely, (either one of the two) Cu−O3, to generate the two copper models, as shown in Chart 2.

Among these, we restricted our attention to model **2b**, which, being constructed by a copper linked to three different pcp's, seems more similar than **2a** to the tin model. Going ahead with the schematization, the carbon and oxygen nodes in both of the models (tin and copper **2b**) were suppressed, to obtain two new skeletons (**1′** and **2′**), respectively characterized by three- and four-membered and three-and six-membered rings (see Figure 7). At this point, the different topology of the two models is just pointed out. However, a further condensation could be performed, by suppressing the three-membered rings. Thus, two models of similar topology were obtained, where the ligand is reduced at a 3-connected point. The new skeletons, **1″** and **2″**, again evidence the difference between the two models, which stems from the different sequence by which the ligand disposes itself with respect to the metal centers (in **1″**, the chelating bite connects the two parallel lines, while in **2″**, it lies on the lines themselves).

^{119}Sn and ^{31}P MAS NMR Spectra of [Sn(pcp)]. The ^{119}Sn MAS NMR spectrum of [Sn(pcp)] shows an isotropic chemical shift at $\delta_{iso} = -685.0$, which is substantially different from that of SnO (−208).[32] In both compounds, the primary coordination sphere of the Sn atoms is defined by four oxygen atoms (CN = 4). The chemical shift difference is consistent with there being significantly more electron density around the tin atom in [Sn(pcp)]. Relatively large anisotropy (ζ) is observed for both [Sn(pcp)] (484) and SnO (654) due to asymmetry in the valence electron cloud about tin.[32] The asymmetry (η) is larger for [Sn(pcp)] (0.40) than for SnO (0.10), with the latter having a 4-fold axis through the tin atom.[32] The ^{31}P MAS NMR shows two signals of equal intensity at 19.5 and 18.3 ppm, indicating the presence of two inequivalent phosphorus atoms, which is consistent with the structure determined by XRPD. These resonances are more deshielded than those of solid H_2pcp (32.8 pp) and the lead analogue, [Pb(pcp)] (24.5 and 31.4 ppm).[16]

Magnetic Properties of [Cu(pcp)]. From a magnetic point of view, [Cu(pcp)] can be regarded as a spin ladder compound, with the rail being the Cu−O−P−O−Cu skeleton and the legs being the O bridge between centrosymmetrically related copper ions. A constant value of $\chi T = 0.44$ emu K mol^{-1} is observed for **2** down to 50 K, as expected for a simple S = 1/2 ion with $g_{ave} \approx 2.19$. This is in agreement with previously reported g values on systems containing similar cromophores[33] and has been confirmed by room temperature X-Band EPR. Indeed, the spectrum clearly shows the axial signal expected for a square pyramidal Cu(II) center, with $g_{||} = 2.40$ and $g_{\perp} = 2.09$ ($g_{ave} = \sqrt{[(2g_{\perp}^2 + g_{||}^2)/3]} = 2.19$), indicating the unpaired electron resides in a $d_{x^2-y^2}$ orbital, as expected on the basis of the structural features.[34] Below 50 K, a decrease in χT is clearly visible, indicating the presence of weak antiferromagnetic interactions (Figure 8). The magnetic data at low temperature were fitted by using two different models. In the first one, we assumed a simple dimer interaction ($\mathbf{H} = J\mathbf{S}_1\mathbf{S}_2$) with molecular field correction to account for the interaction along the rail of the ladder:[35]

$$\chi'_M = \frac{\chi_M}{(1 + (zJ_{mf}/g^2\beta^2)\chi_M)} \qquad (1)$$

Here, J_{mf} is the interdimer interactions, $z = 2$ is the number of nearest neighbors, and χ_M is the dimer susceptibility value calculated as

$$\chi_M = \frac{Ng^2\beta^2}{kT(3 + \exp(J/kT))} \qquad (2)$$

This yielded a fit with best parameter values $g = 2.195 \pm$

(32) Cossement, C.; Darville, J.; Gilles, J. M.; Nagy, J. B.; Fernandez, C.; Amoureux, J. P. *Magn. Reson. Chem.* **1992**, *30*, 263−270.
(33) Cini, R.; Colamarino, P.; Orioli, P. L.; Smith, L. S.; Newman, P. R.; Nannelli, P.; Gillmann, H. D. *Inorg. Chem.* **1977**, *16*, 3223−3226.
(34) Bencini, A.; Gatteschi, D. In *Inorganic electronic structure and spectroscopy*; Lever, A. B. P., Solomon, E. I., Eds.; Wiley-Interscience: New York, 1999.
(35) O'Connor, C. J. *Prog. Inorg. Chem.* **1982**, *29*, 203−283.

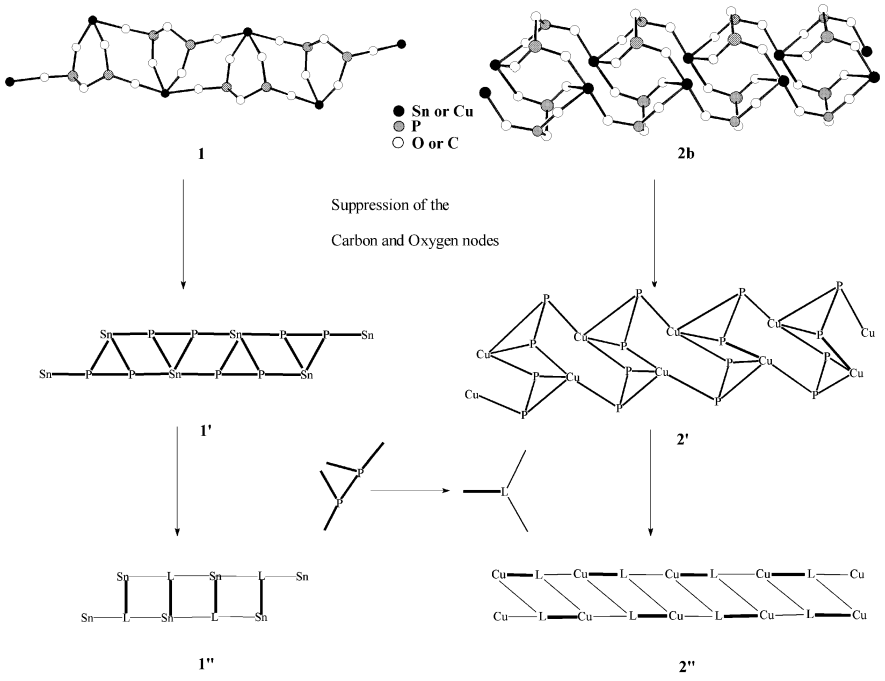

Figure 7. Transformation of the Sn and Cu networks **1** and **2b** into an equivalent 3-connected net. In the first step, the carbon and oxygen nodes (white balls in **1** and **2b**) are suppressed to give two topologically different networks **1′** and **2′**. A further reduction of the pcp ligand into a 3-connected point gives two nets **1″** and **2″**, in which, respectively, the chelating bite of the ligand (represented in bold) connects the two parallel lines or lies on the lines themselves.

0.003, $J = 3.17 \pm 0.04$ cm^{-1}, and $J_{mf} = 0.57 \pm 0.02$ cm^{-1} ($R^2 = \Sigma_i(\chi_{obsd}(i)T_i - \chi_{calcd}(i)T)^2/\chi_{calcd}(i)T_i^2 = 7.6 \times 10^{-6}$). Even if $J/J_{mf} < 10$ so that the molecular field approximation cannot be considered completely valid, the obtained J value for the intradimer coupling is in good agreement with the results of the M vs H curve measured at 1.8 K (Figure 9), which shows a singlet−triplet field induced transition around 4 T, suggesting $J \approx 4$ cm^{-1}.

A more refined model for the fit involved the application of a fourth order polynomial formula, developed for calculating the susceptibility of spin ladders:[36,37]

$$\chi_M = (Ng^2\beta^2/4kT)\left[1 + \frac{1}{kT}\left(-\frac{1}{4}J' - \frac{1}{2}J''\right) + \left(\frac{1}{kT}\right)^2\left(-\frac{1}{16}J'^2 + \frac{1}{4}J'J''\right) + \left(\frac{1}{kT}\right)^3\left(+\frac{1}{192}J'^3 + \frac{1}{32}J'^2J'' - \frac{1}{32}J'^2J'' - \frac{1}{24}J'^3\right) + \left(\frac{1}{kT}\right)^4\left(\frac{5}{768}J'^4 - \frac{1}{48}J'^3J'' + \frac{1}{64}J'^2J''^2 - \frac{1}{48}J'^3J'' + \frac{5}{384}J'^3\right)\right] \quad (3)$$

Here, J' is the leg interaction and J'' is the rail one; best fit curves were obtained with the following parameters: $g = 2.193 \pm 0.002$, $J' = 4.76 \pm 0.03$ cm^{-1}, and $J'' = 0.51 \pm 0.02$ cm^{-1} ($R^2 = 1.45 \times 10^{-6}$). Both fits are of good quality and give essentially the same best fit parameters values. Interestingly, both models reproduce equally well the position and the amplitude of the maximum observed at low temperature in the χ vs T plot (Figure 8, inset). On the other hand, this did not occur if we neglected one of the two exchange-coupling paths, by assuming either a simple dimer model based on eq 2 alone or an isolated chain one based on the

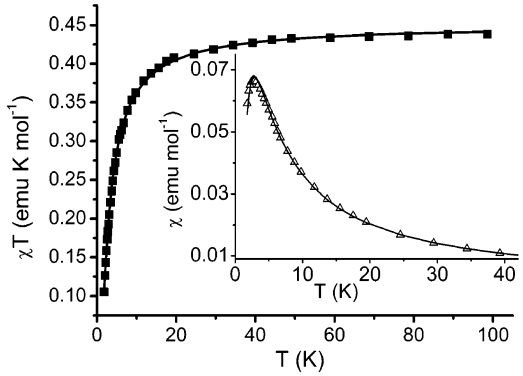

Figure 8. Plot of χT vs T for [Cu(pcp)] and best fit curves obtained on application of the two models (the two best fit curves are indistinguishable). In the inset, the χ vs T plot at low T is reported together with the curves calculated from best fit parameters obtained by fitting χT experimental points.

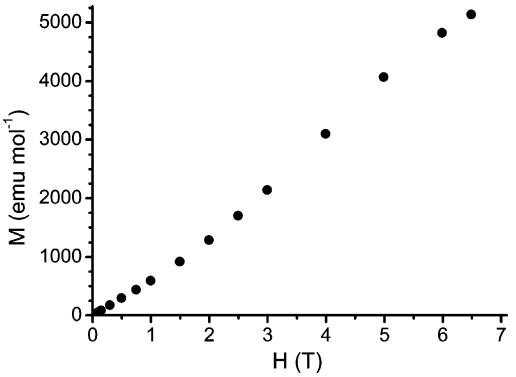

Figure 9. Plot of M vs H curve for [Cu(pcp)], measured at 1.8 K.

(36) Zhou, P.; Drumheller, J. E.; Rubenbacker, G. V.; Halvorson, K.; Willett, R. D. *J. Appl. Phys.* **1991**, *69*, 5804−5806.
(37) Rushbrooke, G. S.; Baker, G. A.; Wood, P. J. In *Phase transition critical phenomena;* Domb, C., Green, M. S., Eds.; Academic Press: New York, 1974; Vol. 3, pp 245−356.

Bonner Fisher expression[38] for isotropic chains. This clearly indicates that both interactions are important in determining the magnetic behavior of **2**.

The observed interaction along the phosphinate group obtained in **2** compares well with what has been reported for similar systems.[39−41] The small value of the constant is probably much the result of different effects counterbalancing each other. Indeed, earlier studies suggested three parameters to govern the sign of magnetic interaction in these kind of systems, namely, the *inter*-ion distance, the planarity of the chromophore, and the puckering of the ring.[39] Analysis of these structural parameters evidences that, while the puckering of the ring is somewhat more pronounced here and the Cu−Cu distance is shorter in **2** than in the ethyl derivatives[39] (4.93 Å vs 4.95 Å and 5.03 Å), the planarity of the chromophore is much more pronounced for **2**. We note here that the main structural feature differentiating **2** from complexes reported in refs 39 and 40 is the value of the dihedral angle between the CuO_4 planes and the O−P−O one, which is much smaller in **2**; we then suggest this might be another relevant parameter influencing the degree of magnetic coupling observed in copper−phosphinate complexes.

As for the intradimer interaction, the small value obtained for the coupling constant is not surprising, despite the short distance separating the two Cu(II) ions, because the magnetic orbital of the two copper ions are unfavorably oriented to give rise to a strong interaction. Indeed, for each copper pair, the oxygen which occupies the basal position of one ion is bound in the axial position to the other one. As the unpaired electron resides in the $d_{x^2-y^2}$ orbital, the degree of delocalization from one site to the other one is then expected to be quite small. In this case, a comparison with ref 40 evidences a stronger interaction for **2**, which can be related both to the much shorter distance between Cu ions (3.1 Å vs 3.6 Å) and to the somewhat shorter $Cu-O_{apical}$ elongation (2.41 Å vs 2.505 Å).

On the basis of this discussion, we can then conclude that both couplings are weak, antiferromagnetic, and in reasonable agreement with reported literature data.[33,39−41]

Acknowledgment. Thanks are expressed to Dr. Samuele Ciattini (Università di Firenze) for the collection of the X-ray powder spectra for[Sn(pcp)].

Supporting Information Available: X-ray crystallographic data in CIF format; Figures S1 and S2, reporting the complete packing diagrams of **1** and **2**, in tiff format.

IC050683P

(38) Kahn, O. In *Molecular magnetism*; Wiley-VCH: New York, 1993.
(39) Haynes, J. S.; Oliver, K. W.; Rettig, S. J.; Thompson, R. C.; Trotter, J. *Can. J. Chem*. **1984**, *62*, 891−898.
(40) Oliver, K. W.; Rettig, S. J.; Thompson, R. C.; Trotter, J.; Xia, S. *Inorg. Chem*. **1997**, *36*, 2465−2468.
(41) Haynes, J. S.; Oliver, K. W.; Thompson, R. C. *Can. J. Chem*. **1985**, *63*, 1111−1117.